

Strong scattering from decay for dark matter freeze-in

Shao-Ping Li^{1,*}

¹*Institute of High Energy Physics, Chinese Academy of Sciences, Beijing 100049, China*

When a nonthermal heavy particle is produced by decays due to the finite-temperature plasma effects, the scattering sharing the same order of couplings with the decay can be activated. Without the suppression of higher-order weak couplings, the scattering effect activated from the kinematically forbidden decay can be much stronger than generically expected. Applying this effect to the freeze-in heavy dark matter production, we find that the dark matter relic density generated through the scattering channel can be several orders of magnitude larger than that from the purely forbidden decay. Such strong effects could be ubiquitous in plasma-induced processes in the early Universe, such as the purely thermal generation of the right-handed neutrino dark matter, or of the lepton asymmetry in leptogenesis.

I. INTRODUCTION

In many theories beyond the Standard Model (SM) of particle physics, a heavy nonthermal species can be usually produced by a light particle in a thermal plasma. This kind of production, which is kinematically forbidden in vacuum but opened at finite temperatures due to plasma effects, has been studied in a wide range of phenomena, such as the dark matter (DM) production [1–7], the neutrino energy emission from the plasmon decay in stars [8–12], and the thermally induced baryon asymmetry in the early Universe [13–24].

In the scenarios of forbidden decay, the two-body scattering mediated by the light particle can also be significant and even dominate the production. A known example is the neutrino chirality-flipping process $\nu_L \rightarrow \nu_R$ in the relativistic QED plasma, where the contribution from the t -channel scattering $e + \nu_L \rightarrow e + \nu_R$ was found to be much larger than that from the plasmon decay $\gamma^* \rightarrow \bar{\nu}_L + \nu_R$, since the latter is suppressed by higher-order electromagnetic coupling α_{EM} [25–28]. A similar effect is also found recently in the electron chirality-flipping process [29, 30]. For a nonthermal DM produced via the freeze-in paradigm [31–35], on the other hand, it has been shown that the forbidden two-body decay can be the dominant mechanism (see e.g., Refs. [1, 5, 36]) and in some cases be the unique channel to account for the DM relic density [6, 7].

The two-body scattering is generically expected to be suppressed by higher-order weak couplings, which results in the two-body decay being the dominant channel for most situations. However, when the decay channel is a purely plasma-induced effect, the two-body scattering activated from the very forbidden decay can carry the same order of coupling constants.

To see this, we show an example in Fig. 1 with the scalar forbidden decay to fermions via the Yukawa interaction $y_\chi \bar{\chi} \chi \phi$. For a vacuum mass condition $m_\phi < 2m_\chi$, the scalar decay $\phi \rightarrow \bar{\chi} + \chi$ is kinematically forbidden in vacuum but opened at temperatures above some critical point $T_c = 2m_\chi/\kappa$, since the light scalar ϕ acquires temperature-

dependent thermal mass $m_\phi(T) \equiv \kappa T$ from e.g., the Yukawa interaction $y_\psi \bar{\psi} \psi \phi$. Here κ characterizes the correction factor from the thermal plasma, which is encoded in the red blob of Fig. 1. Since a nonzero κ is induced by the resummed self-energy in the red blob, it points out that the scattering $\bar{\psi} + \psi \rightarrow \bar{\chi} + \chi$ channel must exist when the forbidden decay is opened. Furthermore, both the scattering and forbidden decay rates carry the same order of coupling prefactor $\propto y_\chi^2 y_\psi^2$, as will be derived below.

Such scattering channels differ from the chirality-flipping process where the plasmon decay is at $\mathcal{O}(\alpha_{\text{EM}}^2)$ while the scattering is at $\mathcal{O}(\alpha_{\text{EM}})$. Without the suppression of higher-order weak coupling constants, the scattering effect could be comparable to the decay rate. In this Letter, we illustrate the importance of the two-body scattering channel, which can exist in a wide range of renormalizable forbidden decay scenarios, such as the millicharged DM [37, 38] generated from the plasmon decay [5], the right-handed neutrino DM [39, 40] from a thermal scalar decay [3], or even a nonthermal DM production from an unknown hidden thermal plasma [41, 42]. The scattering effects could also modify the pattern of leptogenesis when the out-of-equilibrium generation of lepton asymmetries is activated by the forbidden decay in the early Universe [13, 21–24].

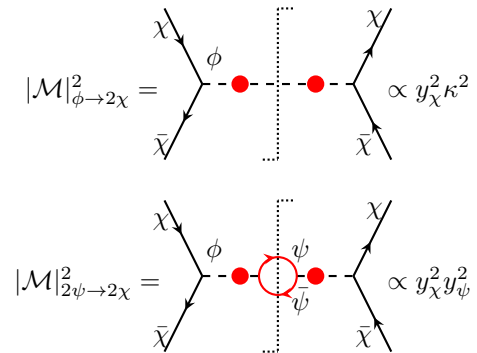


Figure 1. The scattering channel $\bar{\psi} + \psi \rightarrow \bar{\chi} + \chi$ activated from the forbidden decay $\phi \rightarrow \bar{\chi} + \chi$ with the same coupling prefactor $\propto y_\psi^2 y_\chi^2$, where $\kappa \sim y_\psi$ is generically expected when the thermal correction (red blob) to ϕ dominantly arises from a self-energy topology similar to the red one.

* spli@ihep.ac.cn

To illustrate the key formulation for comparing the scattering with the forbidden decay, we consider in the remainder of this Letter the scattering effects in Fig. 1, where the nonthermal fermion χ is a DM candidate having an explicit and direct freeze-in channel from the scalar forbidden decay $\phi \rightarrow \bar{\chi} + \chi$.

As will be shown below, the scattering effect can drastically modify the forbidden decay scenarios of DM production at finite temperatures. In particular, the ratio of the relic density from the scattering to that from the forbidden decay has a simple scaling $\sim 1/y_\psi$ in the weak coupling limit $y_\psi \ll 1$, which can make the DM relic density from the scattering be orders of magnitude larger than that from the pure decay channel.

The investigation presented here complements the widely studied plasma-induced effects at finite temperatures, where the two-body decay and the scattering generically carry different powers of coupling prefactors. While the presentation here is clearly complementary to the studies of decays in a *known* plasma, it can be more attractive and predictive in forbidden channels from a *hidden* thermal plasma.

II. STRONG SCATTERING EFFECTS FROM FORBIDDEN DECAYS

Let us first point out that the scattering effect at high temperatures can be already comparable to the forbidden decay rate. The nonthermal heavy DM χ can be produced by a light thermal scalar ϕ which establishes thermal equilibrium with some light fermion ψ in the plasma. The relevant interaction is characterized by

$$\mathcal{L} = y_\chi \bar{\chi} \chi \phi + y_\psi \bar{\psi} \psi \phi. \quad (1)$$

We consider the situation where thermal particles ϕ, ψ are much lighter than the nonthermal χ at zero temperature so that the nonrelativistic $\bar{\psi}\psi$ annihilation to χ is kinematically forbidden in vacuum. This is applicable to much heavy nonthermal DM production from the thermal plasma. In particular, forbidden decays may open new avenues for superheavy DM production in the early Universe [43, 44]. For simplicity, we further assume that the dominant thermal correction to ϕ can be well encapsulated by the $\bar{\psi}\psi\phi$ interaction. Including other comparable corrections opens additional scattering channels activated from the forbidden decay.

Beyond the Yukawa example given in Eq. (1), however, the activated scattering channel may be evaded in some particular forbidden decay scenario. A typical example is the $\lambda\phi^4$ theory, which generates $\kappa \propto \sqrt{\lambda}$ at leading order [45]. The $\lambda\phi^4$ interaction can also induce a ϕ^3 vertex $\propto \lambda v_\phi$ when ϕ develops a nonzero vacuum expectation value v_ϕ to trigger some spontaneous gauge symmetry breaking. Then, besides the additional dependence on v_ϕ , the scattering rate from $\phi + \phi \rightarrow \bar{\chi} + \chi$ has a higher-order λ prefactor than the forbidden decay $\phi \rightarrow \bar{\chi} + \chi$, and would be suppressed by small λ . Nevertheless, when λ is small, the scattering channel can still be activated from other stronger thermal interactions, e.g., from a trilinear-scalar $\phi\Phi^2$ or a scalar-vector-vector $B_\mu B^\mu \phi$

vertex, unless some symmetry exists to forbid these interactions. Therefore the activated scattering is unavoidable when the dominant thermal correction arises from a self-energy diagram similar to the red bubble in Fig. 1.

From Eq. (1), the squared amplitude in the forbidden decay $\phi \rightarrow \bar{\chi} + \chi$ reads

$$|\mathcal{M}|_{\phi \rightarrow 2\chi}^2 = 2y_\chi^2 (\kappa^2 T^2 - 4m_\chi^2). \quad (2)$$

The Boltzmann equation for the evolution of χ number density is given by

$$\dot{n}_\chi + 3Hn_\chi = 2\gamma_{\phi \rightarrow 2\chi}, \quad (3)$$

where the Hubble parameter reads $H \approx 1.66\sqrt{g_{*,\rho}}T^2/M_{\text{Pl}}$, with $M_{\text{Pl}} = 1.22 \times 10^{19}$ GeV the Planck mass and $g_{*,\rho}$ the effective degrees of freedom for the energy density. The factor 2 results from the χ -pair production. The collision rate from Eq. (2) reads

$$\gamma_{\phi \rightarrow 2\chi} = \frac{\kappa^3 y_\chi^2 K_1(\kappa)}{16\pi^3} \left(1 - \frac{4m_\chi^2}{\kappa^2 T^2}\right)^{3/2} T^4, \quad (4)$$

where $K_1(\kappa)$ is the modified Bessel function with $K_1(\kappa) \approx 1/\kappa$, the Boltzmann distribution $f_\phi = e^{-E_\phi/T}$ is used and the Pauli-blocking effect from the nonthermal DM χ is neglected.

The scattering production for sparse χ occurs through the s -channel $\bar{\psi} + \psi \rightarrow \bar{\chi} + \chi$, while the t channel is suppressed by the phase-space distribution of χ . With the usual treatment in vacuum, the cross section without averaging over the spin degrees of freedom of ψ is simply given by

$$\sigma_{2\psi \rightarrow 2\chi} = \frac{y_\chi^2 y_\psi^2}{4\pi s} \left(1 - \frac{4m_\chi^2}{s}\right)^{3/2}. \quad (5)$$

The resulting collision rate then reads [46]

$$\gamma_{2\psi \rightarrow 2\chi} \approx \frac{T}{32\pi^4} \int_{4m_\chi^2}^{\infty} ds \sigma_{2\psi \rightarrow 2\chi} s^{3/2} K_1(\sqrt{s}/T). \quad (6)$$

It can be seen that, the scattering rate in this vacuum treatment can already be comparable to the forbidden decay rate if κ is at $\mathcal{O}(y_\psi)$. Explicitly, using $\kappa = y_\psi/\sqrt{6}$ to be derived below, we have the approximate relation

$$\gamma_{2\psi \rightarrow 2\chi} \approx 0.3\gamma_{\phi \rightarrow 2\chi} \quad (7)$$

in the massless limit $m_\chi = 0$.

Thus far the cross section is only computed in the limit of $s \gg m_\phi^2(T)$, where the effect near the pole $s = m_\phi^2(T)$ is not taken into account properly. Since the cross section may be enhanced near the pole and both $\gamma_{\phi \rightarrow 2\chi}, \gamma_{2\psi \rightarrow 2\chi}$ have the same prefactor dependence, the effect from such s -channel enhancement could further increase the ratio given by Eq. (7). The resonant enhancement appears when the momentum transfer is at $\mathcal{O}(\kappa T)$. This soft-scattering transfer can come either from the soft $\bar{\psi}\psi$ pair with momenta at

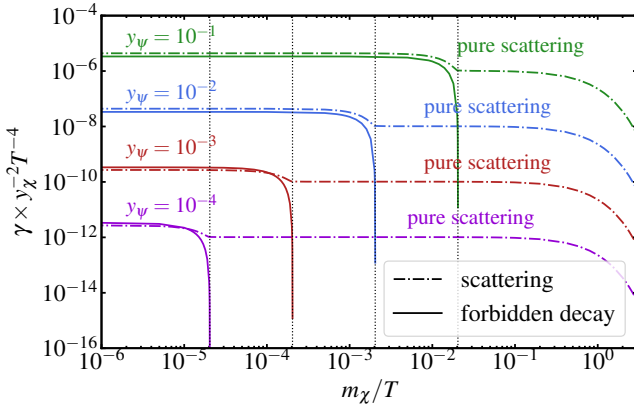


Figure 2. Comparison of collision rates between the forbidden decay and the off-shell scattering. The collision rates are normalized to the squared DM coupling y_χ^2 and the quartic temperature T^4 .

$\mathcal{O}(\kappa T)$, or from the collinear $\bar{\psi}\psi$ pair with hard momenta at $\mathcal{O}(T)$ but with a small angle at $\mathcal{O}(\kappa)$ between the $\bar{\psi}\psi$ momenta [47]. Under the perturbative Hard-Thermal-Loop (HTL) technique [48–50] (see also e.g., Refs. [45, 51]), the thermal correction to ψ for hard $\bar{\psi}\psi$ pair is of higher order, while for soft $\bar{\psi}\psi$ pair, both the thermal correction to ψ and the resummed $\bar{\psi}\psi\phi$ vertex should be included to obtain a consistent result at leading order. Here we consider the hard $\bar{\psi}\psi$ pair for simplicity.

Following the effective treatment in Ref. [47], we compute the cross section by including the leading-order thermal correction in the internal ϕ propagator and treating the external hard $\bar{\psi}\psi$ pair effectively massless. The cross section reads

$$\sigma_{2\psi \rightarrow 2\chi} = \frac{y_\chi^2 y_\psi^2}{4\pi\sqrt{s}} \frac{(s - 4m_\chi^2)^{3/2}}{[s - \text{Re}\Pi_R^\phi]^2 + [\text{Im}\Pi_R^\phi]^2}, \quad (8)$$

where Π_R^ϕ is the resummed retarded self-energy amplitude of ϕ . In the real-time formalism of thermal field theory [52, 53], the real part of Π_R^ϕ is given by

$$\text{Re}\Pi_R^\phi = \frac{y_\psi^2}{\pi^3} \int d^4q f_\psi(\omega) \frac{k \cdot q}{(k+q)^2} \delta(q^2), \quad (9)$$

where $f_\psi(\omega) = (e^{\omega/T} + 1)^{-1}$ is the Fermi-Dirac distribution function for ψ with $\omega \equiv |q_0|$ and k is the 4-momentum of ϕ with $s = k^2$. In the HTL approximation, we disregard the higher-order terms $k^2/|\vec{q}|^2 \sim y_\psi^2$ in the integral and obtain $\text{Re}\Pi_R^\phi \approx y_\psi^2 T^2/6$. The dispersion relation of the thermal scalar ϕ is determined by the pole $k^2 - \text{Re}\Pi_R^\phi = 0$, resulting in $\kappa = y_\psi/\sqrt{6}$. On the other hand, the imaginary self-energy amplitude is given by

$$\text{Im}\Pi_R^\phi = -\frac{y_\psi^2 k^2}{4\pi^2} \int d^4q [1 - 2f_\psi(\omega)] \delta_{k+q} \delta_q, \quad (10)$$

where the two Dirac δ -functions $\delta_{k+q} \equiv \delta[(k+q)^2]$ and $\delta_q \equiv \delta(q^2)$ dictate the on-shell thermal $\psi\psi$ pair. The imaginary

part can be approximated as $\text{Im}\Pi_R^\phi \approx -y_\psi^2 s/(8\pi)$ for hard ψ , which serves to smooth the cross section near the resonance region.

To obtain the off-shell s -channel scattering rate, we take Eq. (8) to the collision rate in Eq. (6), and subtract the on-shell point from the cross section so as to avoid the double counting [47, 54]. The comparison between the forbidden decay and the scattering is shown in Fig. 2. For $T \gg T_c$, the scattering rate dominates for $y_\psi = 10^{-1}, 10^{-2}$, with $\gamma_{2\psi \rightarrow 2\chi} \approx 1.3\gamma_{\phi \rightarrow 2\chi}$. However the enhancement decreases to 0.8 for $y_\psi = 10^{-3}, 10^{-4}$, since the resonant width in the cross section becomes narrower. For all these cases, the relation in Eq. (7) is always lifted up by a factor of $\mathcal{O}(1)$. Therefore the thermal correction included in the propagator can partially compensate for the suppression of additional phase-space factors in the two-body scattering.

When T evolves down to the threshold point $T_c = 2m_\chi/\kappa$, the kinematic space for the forbidden decay tends to close, thereby exhibiting a deep drop in Fig. 2. On the other hand, there is no longer resonant enhancement in the scattering since $s \geq 4m_\chi^2 > m_\phi^2(T)$, resulting in a mild drop in the scattering curve. Nevertheless, the scattering continues until T drops below m_χ , and the scattering rate will carry a Boltzmann suppression factor $e^{-m_\chi/T}$ afterwards, thereby exhibiting a second drop.

Besides an $\mathcal{O}(1)$ enhancement near the resonance, there is a more important effect after the decay channel closes. As seen in Fig. 2, there is a period of χ production from the pure scattering channel and the duration depends on the thermal coupling y_ψ . For smaller y_ψ , the duration is longer and hence more χ production. This is explained by the fact that smaller y_ψ dictates a higher threshold temperature T_c , consequently leading to a shorter duration of the forbidden decay in the early Universe. This observation implies that the contribution from the scattering can be much larger than the forbidden decay if the pure scattering lasts sufficiently long in the expansion history of the Universe.

III. SCATTERING IN FORBIDDEN FREEZE-IN DM

To see the importance of the scattering channel, we solve the Boltzmann equation of the DM number density yield $Y_\chi \equiv n_\chi/s_{\text{SM}}$ from

$$\frac{dY_\chi}{dT} = \int_{T_c}^{\infty} \frac{2\gamma_{\phi \rightarrow 2\chi}}{s_{\text{SM}}HT} dT + \int_0^{\infty} \frac{2\gamma_{2\psi \rightarrow 2\chi}}{s_{\text{SM}}HT} dT, \quad (11)$$

where $s_{\text{SM}} = g_{*,s} 2\pi^2 T^3/45$ is the SM entropy density with $g_{*,s}$ the effective degrees of freedom. The forbidden decay is closed at $T_c = 2m_\chi/\kappa$, and the scattering essentially ends around $T \simeq m_\chi$ but using $T = 0$ as the lower limit in Eq. (11) does not cause significant difference. In the following, we will not distinguish the small difference between $g_{*,s}$ and $g_{*,\rho}$ [55], and simply set $g_{*,s} = g_{*,\rho} = 106.75$ for numerical estimates.

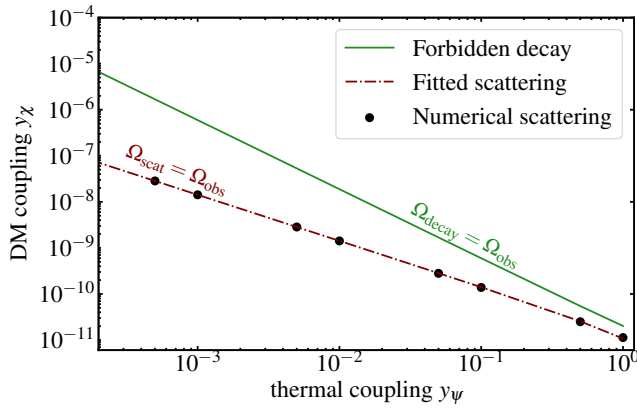


Figure 3. The correlation between the DM coupling y_χ and the thermal coupling y_ψ for the observed DM relic density obtained from the forbidden decay and the scattering channel, respectively. The sampled points denote the numerical scattering rate, which is in agreement with the fitted line within an error of 2%.

To compare the relic densities produced from the forbidden decay and the scattering, we integrate the temperature analytically for $\gamma_{\phi \rightarrow 2\chi}$ and numerically for $\gamma_{2\psi \rightarrow 2\chi}$, where the analytic relic density from the decay channel can be written as

$$\Omega_{\phi \rightarrow 2\chi} h^2 \approx 0.34 \left(\frac{y_\psi}{0.1} \right)^3 \left(\frac{y_\chi}{10^{-9}} \right)^2 \quad (12)$$

for a generically weak coupling $y_\psi \lesssim 1$.

Note that $\Omega_{\phi \rightarrow 2\chi} \propto y_\psi^3$ while $\gamma_{\phi \rightarrow 2\chi} \propto y_\psi^2$. The additional power dependence on the thermal coupling y_ψ comes from the fact that the freeze-in DM production is IR dominated, and both the decay $\phi \rightarrow \bar{\chi} + \chi$ and the annihilation $\bar{\psi} + \psi \rightarrow \bar{\chi} + \chi$ are kinematically forbidden at zero temperature, making the yield Y_χ depend on the inverse threshold temperature and the heavy DM mass scale. It is then observed that we can disentangle $\Omega_{\phi \rightarrow 2\chi}$ from the DM mass [6]. Here we find that this observation also holds for $\Omega_{2\psi \rightarrow 2\chi}$ from the scattering channel. However, for the vacuum mass condition $m_\psi > m_\chi$, the annihilation $2\psi \rightarrow 2\chi$ is opened at zero temperature and the yield Y_χ would not have the simple $1/m_\chi$ dependence. This is the case for the sub-MeV or lighter DM production from the nonrelativistic electron-positron annihilation [5, 36].

Independent of the DM mass, the ratio of $\Omega_{2\psi \rightarrow 2\chi}$ to $\Omega_{\phi \rightarrow 2\chi}$ can then be simply estimated by the thermal coupling y_ψ . Approximately, we find that the ratio can be well fitted as

$$\frac{\Omega_{2\psi \rightarrow 2\chi}}{\Omega_{\phi \rightarrow 2\chi}} \approx 0.8y_\psi + 1.8y_\psi^{-1} + 0.5, \quad (13)$$

where the error is less than 2%. For smaller thermal coupling y_ψ , the ratio basically scales as $1/y_\psi$. Taking $y_\psi = 10^{-3}$ for example, we can see that the DM relic density produced through the scattering channel is a factor of 1800 larger than that through the forbidden decay, however the ratio decreases below $\mathcal{O}(10)$ for a SM electroweak coupling. It implies that the scattering effects can become much stronger than what is

generically expected from the SM, e.g., when the light particle comes from a hidden thermal plasma different from the SM one [41, 42]. We can also see from Fig. 3 the correlation between the nonthermal DM coupling y_χ and the thermal coupling y_ψ when the observed DM relic density $\Omega_{\text{obs}} h^2 = 0.12$ [56] is accounted for by the forbidden decay and the scattering channel, respectively. The sampled points are obtained by numerically integrating $\gamma_{2\psi \rightarrow 2\chi}$ while the solid line is obtained via the analytic formula given in Eq. (13). As seen from Fig. 3, the strong scattering contribution opens up the parameter space of the nonthermal DM coupling towards smaller values.

While we only consider the simplest scalar mediator case here, the strong scattering effect is also expected in other light mediator situations. For instance, a fermion DM coupling to the SM via a vector mediator (the photon) has been considered in Refs. [5, 36]. It was demonstrated that the plasmon decay is the dominant channel for sub-MeV DM production. This can in fact be explained by Fig. 2. The effective photon thermal mass can be estimated by a correction factor $\kappa \sim \sqrt{\alpha_{\text{EW}}} \sim \mathcal{O}(0.1)$ in the thermal plasma. For a sub-MeV DM the threshold temperature can reach $T_c \sim 10^{-3}$ GeV and the deep drop of the decay curve in Fig. 2 can be postponed until $m_\chi/T \simeq \mathcal{O}(0.1)$. When the temperature is above the electron mass m_e , the contributions from the plasmon decay and the electron-positron pair production are comparable. However, the pair production becomes Boltzmann suppressed when $T_c < T < m_e$, and the scattering curve in Fig. 2 would exhibit a second drop prior to the deep drop in the decay curve. In this case, the scattering contribution is suppressed in the history of the production and the plasmon decay becomes the dominant channel. For much heavier DM, however, the production from the nonrelativistic electron-positron annihilation is kinematically forbidden. In this case, the collision rates from the plasmon decay and the electron-positron scattering are expected to have similar patterns shown in Fig. 2.

The activated scattering effect can also have important consequences in the scenarios of right-handed neutrino DM production [3, 57]. When the right-handed neutrino N_R is nonthermally produced by some forbidden decay at higher temperatures, the contribution from the activated scattering sensitively depends on the mediator connecting the SM and N_R . If the mediator is the SM Higgs, the forbidden Higgs decay $H \rightarrow \ell + N_R$ is generically opened to generate heavy N_R as well as the SM leptons ℓ at much higher temperatures [13]. However, since the Higgs boson carries $\kappa \approx 0.4$ [58] from gauge and top Yukawa interactions, Fig. 3 or Eq. (13) implies that the s -channel scattering from e.g. the top-quark pair $\bar{t} + t \rightarrow \ell + N_R$ would not drastically increase the production rate from the forbidden Higgs decay $H \rightarrow \ell + N_R$. This conclusion is consistent with earlier observations [13]. Instead of the SM Higgs mediator, if N_R has interactions from Eq. (1), the nonthermal DM production from the forbidden decay $\phi \rightarrow 2N_R$ can be boosted by the $2\psi \rightarrow 2N_R$ channel.

The out-of-equilibrium scattering production activated from the forbidden decay can also modify the thermally in-

duced generation of lepton asymmetries in the early Universe, if N_R participates in the leptogenesis scenarios [13, 21–24]. If the nonthermal forbidden decay to N_R from some light mediator is CP violated, the CP asymmetry stored in N_R can be transferred to the SM one, which in the active sphaleron epoch is partially converted into the baryon asymmetry. If the mediator carries a correction factor $\kappa \ll 1$ from the thermal plasma, the scattering channel can be readily stronger than the forbidden decay.

IV. CONCLUSION

We have illustrated a novel feature of the scattering channel that is activated by the forbidden decay at finite temperatures. Instead of carrying higher-order weak coupling constants as generically expected, the two-body scattering activated from the very forbidden decay can carry the same order of coupling constants. An $\mathcal{O}(1)$ enhancement in the s -channel scat-

tering rate arises when the thermal corrections are included in the mediator propagator. A more tremendous effect from the scattering contribution is illustrated via the freeze-in DM production from a direct forbidden decay, where the enhancement of the DM relic density from the scattering channel can readily reach orders of magnitude. This can be realized when the light particle is a gauge singlet of the SM or comes from a hidden thermal plasma. We have also discussed the potential impacts on the right-handed neutrino DM production and leptogenesis.

ACKNOWLEDGMENTS

The author thanks Oleg Lebedev, Katelin Schutz and Xunjie Xu for valuable discussions. This work is supported in part by the National Natural Science Foundation of China under grant No. 12141501.

-
- [1] V. S. Rychkov and A. Strumia, *Thermal production of gravitinos*, *Phys. Rev. D* **75** (2007) 075011, [[hep-ph/0701104](#)].
 - [2] A. Strumia, *Thermal production of axino Dark Matter*, *JHEP* **06** (2010) 036, [[arXiv:1003.5847](#)].
 - [3] M. Drewes and J. U. Kang, *Sterile neutrino Dark Matter production from scalar decay in a thermal bath*, *JHEP* **05** (2016) 051, [[arXiv:1510.05646](#)].
 - [4] M. J. Baker, M. Breitbach, J. Kopp, and L. Mittnacht, *Dynamic Freeze-In: Impact of Thermal Masses and Cosmological Phase Transitions on Dark Matter Production*, *JHEP* **03** (2018) 114, [[arXiv:1712.03962](#)].
 - [5] C. Dvorkin, T. Lin, and K. Schutz, *Making dark matter out of light: freeze-in from plasma effects*, *Phys. Rev. D* **99** (2019), no. 11 115009, [[arXiv:1902.08623](#)]. [Erratum: *Phys.Rev.D* 105, 119901 (2022)].
 - [6] L. Darmé, A. Hryczuk, D. Karamitros, and L. Roszkowski, *Forbidden frozen-in dark matter*, *JHEP* **11** (2019) 159, [[arXiv:1908.05685](#)].
 - [7] P. Konar, R. Roshan, and S. Show, *Freeze-in dark matter through forbidden channel in $U(1)_{B-L}$* , *JCAP* **03** (2022), no. 03 021, [[arXiv:2110.14411](#)].
 - [8] J. Bernstein, M. Ruderman, and G. Feinberg, *Electromagnetic Properties of the neutrino*, *Phys. Rev.* **132** (1963) 1227–1233.
 - [9] E. Braaten and D. Segel, *Neutrino energy loss from the plasma process at all temperatures and densities*, *Phys. Rev. D* **48** (1993) 1478–1491, [[hep-ph/9302213](#)].
 - [10] G. G. Raffelt, *Stars as laboratories for fundamental physics: The astrophysics of neutrinos, axions, and other weakly interacting particles*. University of Chicago Press, 1996.
 - [11] D. G. Yakovlev, A. D. Kaminker, O. Y. Gnedin, and P. Haensel, *Neutrino emission from neutron stars*, *Phys. Rept.* **354** (2001) 1, [[astro-ph/0012122](#)].
 - [12] E. Hardy and R. Lasenby, *Stellar cooling bounds on new light particles: plasma mixing effects*, *JHEP* **02** (2017) 033, [[arXiv:1611.05852](#)].
 - [13] G. F. Giudice, A. Notari, M. Raidal, A. Riotto, and A. Strumia, *Towards a complete theory of thermal leptogenesis in the SM and MSSM*, *Nucl. Phys.* **B685** (2004) 89–149, [[hep-ph/0310123](#)].
 - [14] M. Garny, A. Hohenegger, A. Kartavtsev, and M. Lindner, *Systematic approach to leptogenesis in nonequilibrium QFT: Self-energy contribution to the CP-violating parameter*, *Phys. Rev. D* **81** (2010) 085027, [[arXiv:0911.4122](#)].
 - [15] M. Garny, A. Hohenegger, A. Kartavtsev, and M. Lindner, *Systematic approach to leptogenesis in nonequilibrium QFT: Vertex contribution to the CP-violating parameter*, *Phys. Rev. D* **80** (2009) 125027, [[arXiv:0909.1559](#)].
 - [16] C. P. Kiessig, M. Plumacher, and M. H. Thoma, *Decay of a Yukawa fermion at finite temperature and applications to leptogenesis*, *Phys. Rev. D* **82** (2010) 036007, [[arXiv:1003.3016](#)].
 - [17] M. Garny, A. Hohenegger, and A. Kartavtsev, *Medium corrections to the CP-violating parameter in leptogenesis*, *Phys. Rev. D* **81** (2010) 085028, [[arXiv:1002.0331](#)].
 - [18] C. Kiessig and M. Plumacher, *Hard-Thermal-Loop Corrections in Leptogenesis I: CP-Asymmetries*, *JCAP* **07** (2012) 014, [[arXiv:1111.1231](#)].
 - [19] C. Kiessig and M. Plumacher, *Hard-Thermal-Loop Corrections in Leptogenesis II: Solving the Boltzmann Equations*, *JCAP* **09** (2012) 012, [[arXiv:1111.1235](#)].
 - [20] B. Garbrecht, *Leptogenesis from Additional Higgs Doublets*, *Phys. Rev. D* **85** (2012) 123509, [[arXiv:1201.5126](#)].
 - [21] T. Hambye and D. Teresi, *Higgs doublet decay as the origin of the baryon asymmetry*, *Phys. Rev. Lett.* **117** (2016), no. 9 091801, [[arXiv:1606.00017](#)].
 - [22] T. Hambye and D. Teresi, *Baryogenesis from L-violating Higgs-doublet decay in the density-matrix formalism*, *Phys. Rev. D* **96** (2017), no. 1 015031, [[arXiv:1705.00016](#)].
 - [23] S.-P. Li, X.-Q. Li, X.-S. Yan, and Y.-D. Yang, *Freeze-in Dirac neutrino genesis: thermal leptonic CP asymmetry*, *Eur. Phys. J. C* **80** (2020), no. 12 1122, [[arXiv:2005.02927](#)].

- [24] S.-P. Li, X.-Q. Li, X.-S. Yan, and Y.-D. Yang, *Baryogenesis from hierarchical Dirac neutrinos*, *Phys. Rev. D* **104** (2021), no. 11 115014, [[arXiv:2105.01317](#)].
- [25] M. Fukugita and S. Yazaki, *Reexamination of Astrophysical and Cosmological Constraints on the Magnetic Moment of Neutrinos*, *Phys. Rev. D* **36** (1987) 3817.
- [26] P. Elmfors, K. Enqvist, G. Raffelt, and G. Sigl, *Neutrinos with magnetic moment: Depolarization rate in plasma*, *Nucl. Phys. B* **503** (1997) 3–23, [[hep-ph/9703214](#)].
- [27] A. Ayala, J. C. D’Olivo, and M. Torres, *Right-handed neutrino production in dense and hot plasmas*, *Nucl. Phys. B* **564** (2000) 204–222, [[hep-ph/9907398](#)].
- [28] S.-P. Li and X.-J. Xu, *Neutrino Magnetic Moments Meet Precision N_{eff} Measurements*, [arXiv:2211.04669](#).
- [29] A. Boyarsky, V. Cheianov, O. Ruchayskiy, and O. Sobol, *Evolution of the Primordial Axial Charge across Cosmic Times*, *Phys. Rev. Lett.* **126** (2021), no. 2 021801, [[arXiv:2007.13691](#)].
- [30] A. Boyarsky, V. Cheianov, O. Ruchayskiy, and O. Sobol, *Equilibration of the chiral asymmetry due to finite electron mass in electron-positron plasma*, *Phys. Rev. D* **103** (2021), no. 1 013003, [[arXiv:2008.00360](#)].
- [31] J. McDonald, *Thermally generated gauge singlet scalars as selfinteracting dark matter*, *Phys. Rev. Lett.* **88** (2002) 091304, [[hep-ph/0106249](#)].
- [32] A. Kusenko, *Sterile neutrinos, dark matter, and the pulsar velocities in models with a Higgs singlet*, *Phys. Rev. Lett.* **97** (2006) 241301, [[hep-ph/0609081](#)].
- [33] K. Petraki and A. Kusenko, *Dark-matter sterile neutrinos in models with a gauge singlet in the Higgs sector*, *Phys. Rev. D* **77** (2008) 065014, [[arXiv:0711.4646](#)].
- [34] L. J. Hall, K. Jedamzik, J. March-Russell, and S. M. West, *Freeze-In Production of FIMP Dark Matter*, *JHEP* **03** (2010) 080, [[arXiv:0911.1120](#)].
- [35] N. Bernal, M. Heikinheimo, T. Tenkanen, K. Tuominen, and V. Vaskonen, *The Dawn of FIMP Dark Matter: A Review of Models and Constraints*, *Int. J. Mod. Phys. A* **32** (2017), no. 27 1730023, [[arXiv:1706.07442](#)].
- [36] J. H. Chang, R. Essig, and A. Reinert, *Light(ly)-coupled Dark Matter in the keV Range: Freeze-In and Constraints*, *JHEP* **03** (2021) 141, [[arXiv:1911.03389](#)].
- [37] S. Davidson, S. Hannestad, and G. Raffelt, *Updated bounds on millicharged particles*, *JHEP* **05** (2000) 003, [[hep-ph/0001179](#)].
- [38] J. H. Chang, R. Essig, and S. D. McDermott, *Supernova 1987A Constraints on Sub-GeV Dark Sectors, Millicharged Particles, the QCD Axion, and an Axion-like Particle*, *JHEP* **09** (2018) 051, [[arXiv:1803.00993](#)].
- [39] M. Drewes et al., *A White Paper on keV Sterile Neutrino Dark Matter*, *JCAP* **01** (2017) 025, [[arXiv:1602.04816](#)].
- [40] A. Boyarsky, M. Drewes, T. Lasserre, S. Mertens, and O. Ruchayskiy, *Sterile neutrino Dark Matter*, *Prog. Part. Nucl. Phys.* **104** (2019) 1–45, [[arXiv:1807.07938](#)].
- [41] J. L. Feng, H. Tu, and H.-B. Yu, *Thermal Relics in Hidden Sectors*, *JCAP* **10** (2008) 043, [[arXiv:0808.2318](#)].
- [42] A. Berlin, D. Hooper, and G. Krnjaic, *Thermal Dark Matter From A Highly Decoupled Sector*, *Phys. Rev. D* **94** (2016), no. 9 095019, [[arXiv:1609.02555](#)].
- [43] D. J. H. Chung, E. W. Kolb, and A. Riotto, *Superheavy dark matter*, *Phys. Rev. D* **59** (1998) 023501, [[hep-ph/9802238](#)].
- [44] D. J. H. Chung, P. Crotty, E. W. Kolb, and A. Riotto, *On the Gravitational Production of Superheavy Dark Matter*, *Phys. Rev. D* **64** (2001) 043503, [[hep-ph/0104100](#)].
- [45] M. Bellac, *Thermal Field Theory*. Cambridge University Press, 2000.
- [46] P. Gondolo and G. Gelmini, *Cosmic abundances of stable particles: Improved analysis*, *Nucl. Phys. B* **360** (1991) 145–179.
- [47] P. B. Arnold, G. D. Moore, and L. G. Yaffe, *Effective kinetic theory for high temperature gauge theories*, *JHEP* **01** (2003) 030, [[hep-ph/0209353](#)].
- [48] E. Braaten and R. D. Pisarski, *Soft Amplitudes in Hot Gauge Theories: A General Analysis*, *Nucl. Phys. B* **337** (1990) 569–634.
- [49] J. Frenkel and J. C. Taylor, *High Temperature Limit of Thermal QCD*, *Nucl. Phys. B* **334** (1990) 199–216.
- [50] E. Braaten and R. D. Pisarski, *Simple effective Lagrangian for hard thermal loops*, *Phys. Rev. D* **45** (1992), no. 6 R1827.
- [51] M. E. Carrington, D.-f. Hou, and M. H. Thoma, *Equilibrium and nonequilibrium hard thermal loop resummation in the real time formalism*, *Eur. Phys. J. C* **7** (1999) 347–354, [[hep-ph/9708363](#)].
- [52] N. P. Landsman and C. G. van Weert, *Real and Imaginary Time Field Theory at Finite Temperature and Density*, *Phys. Rept.* **145** (1987) 141.
- [53] J. Ghiglieri, A. Kurkela, M. Strickland, and A. Vuorinen, *Perturbative Thermal QCD: Formalism and Applications*, *Phys. Rept.* **880** (2020) 1–73, [[arXiv:2002.10188](#)].
- [54] V. De Romeri, D. Karamitros, O. Lebedev, and T. Toma, *Neutrino dark matter and the Higgs portal: improved freeze-in analysis*, *JHEP* **10** (2020) 137, [[arXiv:2003.12606](#)].
- [55] L. Husdal, *On Effective Degrees of Freedom in the Early Universe*, *Galaxies* **4** (2016), no. 4 78, [[arXiv:1609.04979](#)].
- [56] **Planck** Collaboration, N. Aghanim et al., *Planck 2018 results. VI. Cosmological parameters*, *Astron. Astrophys.* **641** (2020) A6, [[arXiv:1807.06209](#)]. [Erratum: *Astron. Astrophys.* 652, C4 (2021)].
- [57] D. Besak and D. Bodeker, *Thermal production of ultrarelativistic right-handed neutrinos: Complete leading-order results*, *JCAP* **03** (2012) 029, [[arXiv:1202.1288](#)].
- [58] J. M. Cline, K. Kainulainen, and K. A. Olive, *Protecting the primordial baryon asymmetry from erasure by sphalerons*, *Phys. Rev. D* **49** (1994) 6394–6409, [[hep-ph/9401208](#)].